Relationship between morphology and properties of polyamide-6 low-density polyethylene blends: effect of the addition of functionalized low-density polyethylene

Heta Raval and Surekha Devi*
Department of Chemistry, Faculty of Science, M.S. University of Baroda, Baroda 390 002, India

Y. P. Singh and M. H. Mehta
Research and Development Centre, Gujarat State Fertilizer Co. Ltd, Baroda, India
(Received 7 July 1989; revised 5 December 1989; accepted 23 February 1990)

Binary and ternary blends of polyamide-6/low-density polyethylene (PA-6/LDPE) and PA-6/LDPE/LDPE-*g*-butyl acrylate were prepared by melt mixing. The blends were characterized for their various mechanical properties and extent of water absorption. Morphology of the prepared blends was studied by scanning electron microscopy. It was observed that the use of LDPE-*g*-butyl acrylate as an interfacial agent improves the impact strength of PA-6 and decreases the water absorption remarkably.

(Keywords: blends; compatibility; grafting; morphology; impact strength)

INTRODUCTION

Polymer blends are a solution to industry's ever growing demand for polymeric materials having a desirable combination of properties at lower cost. Blending has been done for years to improve the performance of commodity and engineering plastics to achieve wider applications. Polyamide-6 (PA-6) is a polymer of great industrial importance, but it has limitations in its end use because of its (i) low impact strength particularly below the glass transition temperature, (ii) poor dimensional stability due to high moisture pick-up and (iii) poor processability. The impact strength of PA-6 may be improved by blending it with an elastomer having lower T_g. But for efficient improvement of the properties the elastomeric particles must be homogeneously dispersed and must adhere well to the matrix. This may be achieved by using interfacial agents. In several patents the use of polyolefin as a property modifier for PA-6 has been reported[1–4]. Blending of PA-6 with polyolefin leads to a thermodynamically immiscible two-phase system. Braun and Eisenlohr[5] have used dynamic mechanical testing and microscopy to show the presence of two phases in blends of low-density polyethylene (LDPE) with PA-6. Liang *et al.*[6] have observed the incompatibility of polypropylene (PP) with PA-6 and consequently difficulty in dispersion of one in the other.

Ide and Hasegawa[7] achieved compatibility in PA-6/PP blends by using PP-*g*-maleic anhydride as interfacial agent. The improvement in the compatibility was attributed to the formation of PP/PA-6 graft copolymer during melt mixing. The blends prepared by the proper combination of PA-6 and PP-*g*-maleic anhydride were found to have excellent mechanical properties. A similar approach has been followed by Martuscelli *et al.*[8,9] for PA-6/EPM (ethylene–propylene copolymer) blends. They observed that the addition of EPM-*g*-maleic anhydride to blends increased the homogeneity of the blends but decreased the crystallization rate sharply. Similar observations were made by Okada *et al.*[10]. Takashi[11] has reported excellent improvement in the impact strength of PA-6 by blending it with PP-*g*-acrylic acid.

In the present paper we have tried to improve the properties of PA-6. LDPE is tough, flexible and insensitive to moisture and hence is selected as the dispersed phase. To improve the compatibility between PA-6 and LDPE, LDPE-*g*-butyl acrylate (BuA) is used as the interfacial agent.

In the present paper we report the results of detailed investigations of such blends concerning the following aspects.

(i) The study of the influence of the content of LDPE on the overall morphology of injection-moulded PA-6/LDPE and PA-6/LDPE/LDPE-*g*-butyl acrylate blends.

(ii) The correlation between the experimental elastic modulus values with those theoretical (predicted) values derived from various proposed theoretical models.

(iii) The correlation of the overall morphology of binary and ternary blends with tensile mechanical properties and with Izod impact strength at room temperature.

THEORETICAL BACKGROUND

Many theories have been put forward for predicting the elastic modulus of heterogeneous blends. According to Dickie[12] there are three principal groups of models that can predict the modulus–composition dependence for

* To whom correspondence should be addressed

0032-3861/91/030493-08

blends: (1) mechanical coupling model, (2) self-consistent model and (3) 'bounds on modulus' model.

Mechanical coupling model

The mechanical model is an empirical expression containing an adjustable parameter. However, they are not morphological or mechanically realistic models of blend structures.

Self-consistent model

The self-consistent model is based on the following assumptions: (i) perfect adhesion exists between the matrix and the inclusions; (ii) inter-inclusion interactions are negligible; (iii) the inclusions are spherical in shape. According to Kerner's[13] model based on the above assumption, when two polymeric systems have the same Poisson's ratio v and perfect adhesion at the boundary, the tensile modulus of blend is given by:

$$E_b = E_m \frac{\phi_d E_d/[(7-5v_m)+(8-10v_m)E_d] + \phi_m/15(1-v_m)}{\phi_d E_m/[(7-5v_m)+(8-10v_m)E_d] + \phi_m/15(1-v_m)} \quad (1)$$

The Poisson's ratio of PA-6 and LDPE is 0.4 and 0.46 respectively. These values are close enough to use the Kerner equation in the above form for PA-6/LDPE blends and alloys. The terms in equation (1) have the standard notations[13]. E is the tensile modulus, ϕ is the volume fraction of the discrete phase, and v is the Poisson's ratio. The subscripts b, m and d refer to blend, the matrix and the dispersed phase respectively.

For blends in which inclusions are loosely bound, $E_d \simeq 0$, equation (1) reduces to:

$$\frac{1}{E_b} = \frac{1}{E_m}\left[1 + \frac{15(1-v_m)\phi_d}{(7-5v_m)\phi_m}\right] \quad (2)$$

In Kerner's model no particle–particle interaction is considered. Nielson has proposed a modification of Kerner's model. According to him[14] for rubber inclusions in a rigid matrix:

$$\frac{E_m}{E_b} = \frac{1 + AB_i\phi_d}{1 - B_i\phi_d\psi} \quad (3)$$

where

$$B_i = \left(\frac{E_m}{E_d} - 1\right)\Big/\left(\frac{E_m}{E_d} + A\right) \qquad \psi = 1 + \left(\frac{1-\phi_{max}}{\phi_{max}^2}\right)\phi_d$$

and ϕ_{max} is the maximum packing volume and can be considered as a scale of interaction between two phases. The constant A is $(8-10v_m)/(7-5v_m)$.

The 'bounds on modulus' model

The 'bounds on modulus' model defines the limits of the blend moduli. According to Paul[15] the upper limit is given by:

$$E_b = (1-\phi_d)E_m + \phi_d E_d \quad (4)$$

and lower limit by:

$$E_b = 1\Big/\left(\frac{1-\phi_d}{E_m} + \frac{\phi_d}{E_d}\right) \quad (5)$$

We have used all these models for predicting the modulus of PA-6/LDPE blends theoretically.

EXPERIMENTAL

Materials

PA-6 with molecular weight 25 000 and melt flow index 0.5 g/10 min was from Gujarat State Fertilizer Co. Ltd, Baroda, India. LDPE with molecular weight 52 000 and melt flow index 0.2 g/10 min was from Indian Petrochemicals Ltd, Baroda, India.

Details about the synthesis of LDPE-*g*-butyl acrylate (LDPE-*g*-BuA) used as an interfacial agent in the preparation of blends have been reported earlier[16]. Graft copolymer with 17.6 wt% of butyl acrylate was used for the preparation of blends.

Development of the blends

A Haake Rheometer System–40 coupled with a single-screw extruder ($L/D = 16$) was used for the preparation of blends. All the tests were controlled and processed by the software of the Haake system. Master pellets of LDPE-*g*-BuA powder were made by extrusion prior to use. PA-6 granules were dried at 70°C for 48 h prior to use. All the binary blends were prepared by a one-step mixing process and the ternary blends by a two-step mixing process.

One-step mixing technique for binary blends

In this technique all the reactants were mixed in one step. Mixing was carried out in an extruder, keeping the temperature of the three zones at 220°C, 250°C and 260°C and the die temperature at 250°C. The screw speed was 30 rpm.

Two-step mixing technique for ternary blends

The mixing of the reactants was carried out in two steps. In the first step LDPE and LDPE-*g*-BuA were premixed in the extruder, keeping the temperature of the three zones at 140°C, 160°C and 185°C and the die temperature at 140°C. Screw speed was kept at 30 rpm. The resultant mixture was then mixed with PA-6 in the extruder, keeping all the extruder conditions the same as in one-step mixing. All the blends were re-extruded to ensure proper mixing. The various compositions used for the blends under investigation are reported in *Table 1*.

The compounded pellets were injection moulded to obtain test specimens for measurements of tensile properties, Izod impact strength, thermal properties and water absorption.

Table 1 Various compositions of blends

Code no.	PA-6 (%)	LDPE (%)	Modifier (%)
I	100.0	–	–
II	92.7	4.9	2.4
III	87.8	9.8	2.4
IV	82.9	14.7	2.4
V	80.5	17.1	2.4
VI	78.1	19.5	2.4
VII	73.2	24.4	2.4
VIII	68.3	29.3	2.4
IX	95	5	–
X	90	10	–
XI	85	15	–
XII	82.5	17.5	–
XIII	80	20	–
XIV	75	25	–

Tensile property measurements

Tensile property measurements were carried out on an Instron machine at room temperature following the procedure described in ASTM D638. A crosshead speed of 0.5 cm min^{-1} was used in all measurements.

Izod impact strength measurement

All the specimens had dimensions 6.35 × 1.27 × 0.635 cm^3 with a notch of 0.025 cm radius. Impact strength was measured following the procedure described in ASTM D256.

Flexural strength measurement

The measurements were carried out following the procedure described in ASTM D790. A three-point loading system utilizing central loading on a singly supported beam was used for the measurement. A crosshead speed of 0.28 cm min^{-1} was used in all measurements.

Water absorption measurement

All the specimens used for the study had dimensions of about 5.4 × 1.8 × 0.3 cm^3. The test samples were dried at 50°C for 24 h prior to measurements. The samples were first cooled, weighed and then placed in a container of boiling distilled water, supported on edge and entirely immersed in water. After 2 h the specimens were removed from water and cooled in distilled water maintained at room temperature. After 15 min the specimens were removed from water, wiped with a dry cloth and weighed immediately. Percentage of water absorption was determined as follows:

$$\text{percentage water absorption} = \frac{\text{weight of wet sample} - \text{conditioned weight}}{\text{conditioned weight}} \times 100$$

Rockwell hardness measurement

The Rockwell hardness measurement was carried out according to the method described in ASTM D785. Major load of 60 kg and minor load of 10 kg was applied perpendicular to the moulding sample dimensions. Rockwell hardness scale R was used for the hardness measurement.

The Vicat softening temperature (*VST*) and heat distortion temperature (*HDT*) were measured according to ASTM D1525 and ASTM D648 respectively.

Torque measurement

The torque developed during the mixing of PA-6 and LDPE (or modified LDPE) was measured by the Haake Rheometer System-40 coupled with a mixing chamber (Rheomix 600). The measurements of torque *versus* time were recorded on a microprocessor unit. The temperature of the mixer wall was programmed at 260°C. The rotor speed and residence time of the polymer inside the mixing chamber were kept at 30 rpm and 21 min respectively. All the tests were controlled and processed by the software of the Haake system.

Microscopy

The fracture topographs as well as the dispersed structure of the fractured specimens were studied using a scanning electron microscope (JEOL 15) operated at 15–25 kV. The surfaces of the impact-fractured specimens were coated with gold to avoid charging under an electron beam.

RESULTS AND DISCUSSION

When LDPE-*g*-BuA copolymer is added to PA-6/LDPE blends, the following reaction may take place between the ester group of butyl acrylate and the amine group of PA-6 during melt mixing of PA-6 and LDPE-*g*-BuA at 260°C:

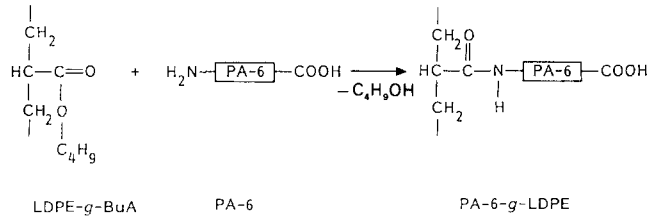

From *Figures 1* and *2* it is observed that PA-6/LDPE blends have LDPE particles uniformly distributed throughout the PA-6 matrix, with particle size of about 20 μm.

As the surface of the dispersed particle is very smooth, it can be concluded that there is no adhesion at the PA-6/LDPE interface.

For PA-6/LDPE/LDPE-*g*-BuA blends (*Figure 3*) a remarkable reduction in particle size of LDPE is observed. It is also to be noted that the LDPE particle has a rough surface, owing to increased adhesion between LDPE particles and PA-6 matrix. This observation indicates that in PA-6/LDPE/LDPE-*g*-BuA blends the LDPE-*g*-BuA acts as an 'interfacial agent' promoting adhesion between matrix and dispersed phase.

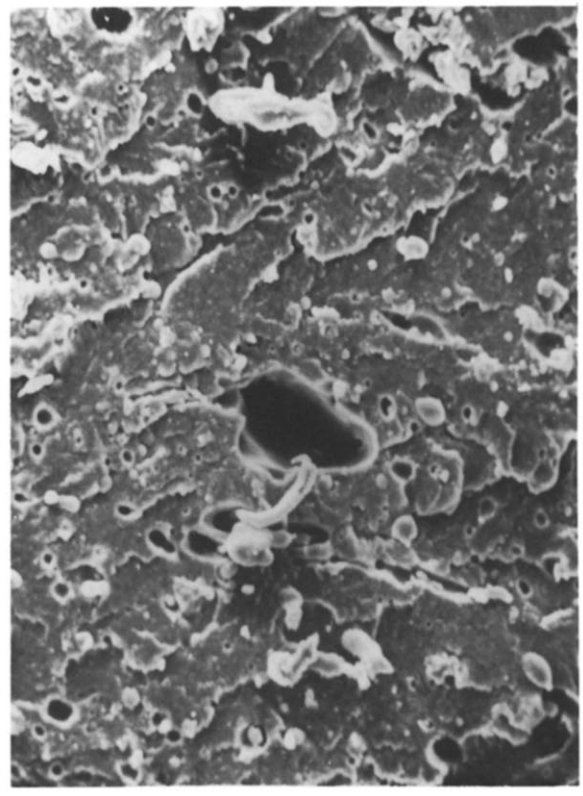

Figure 1 SEM micrograph of an Izod fracture surface of PA-6/LDPE (X) blend (200×)

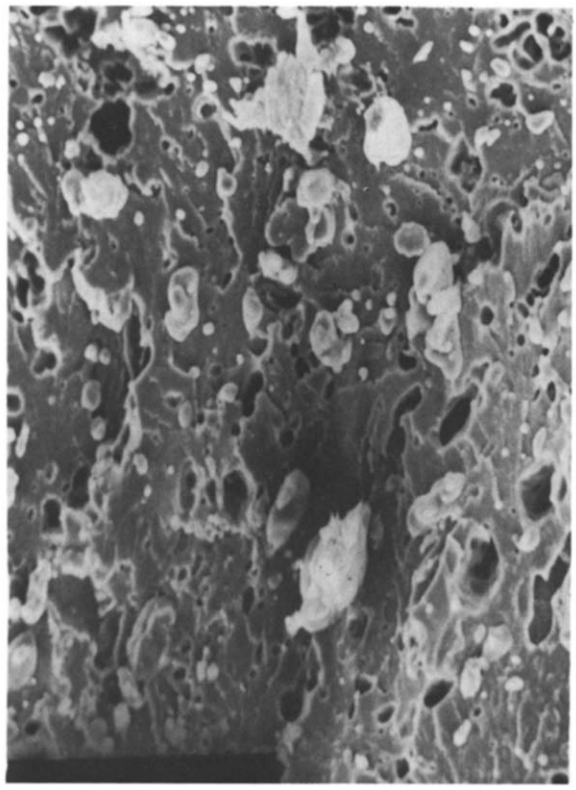

Figure 2 SEM micrograph of an Izod fracture surface of PA-6/LDPE (XIV) blend (200×)

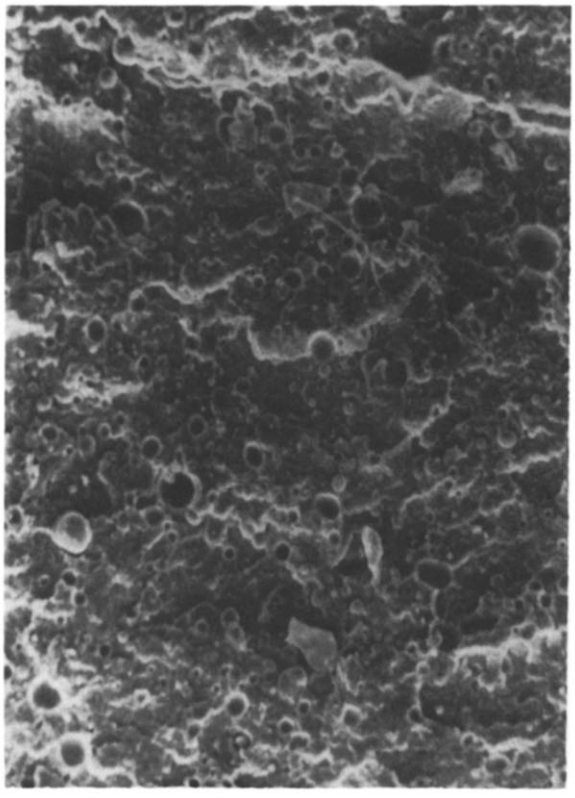

Figure 3 SEM micrograph of an Izod fracture surface of PA-6/LDPE/LDPE-*g*-BuA (II) blend (200×)

On addition of formic acid to PA-6/LDPE blends, a satisfactory separation of PA-6 from LDPE was observed, whereas the PA-6/LDPE/LDPE-*g*-BuA blends give rise to colloidal solutions in formic acid. According to Molau[17] this result can be taken as an indication that PA-6-*g*-LDPE is present in PP-6/LDPE/LDPE-*g*-BuA blends acting as an interfacial agent.

Tensile mechanical properties

Stress–strain curves for PA-6/LDPE/LDPE-*g*-BuA blends are shown in *Figure 4*. It is seen that PA-6 shows necking behaviour, while in the blend with increasing LDPE content necking decreases. From *Figure 5* it can be observed that tensile modulus values of all the blends are lower than those of PA-6. As the tensile modulus of

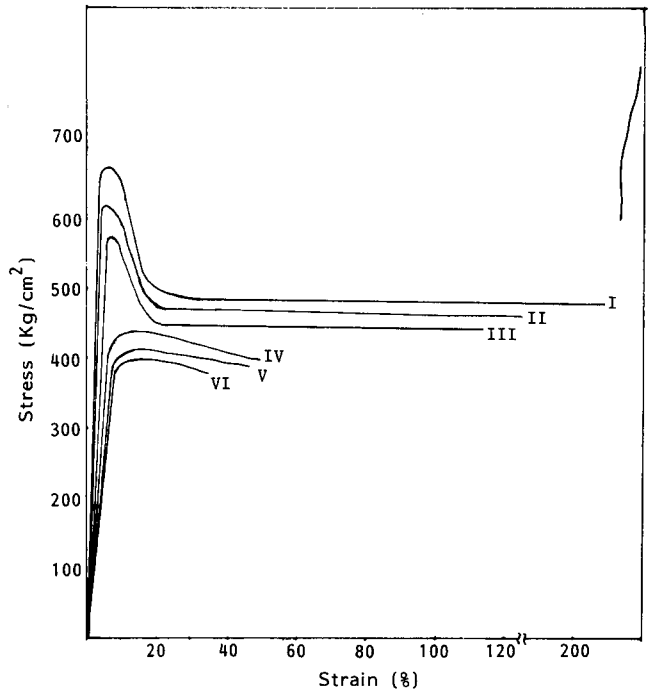

Figure 4 Stress–strain curves for PA-6/LDPE/LDPE-*g*-BuA blends

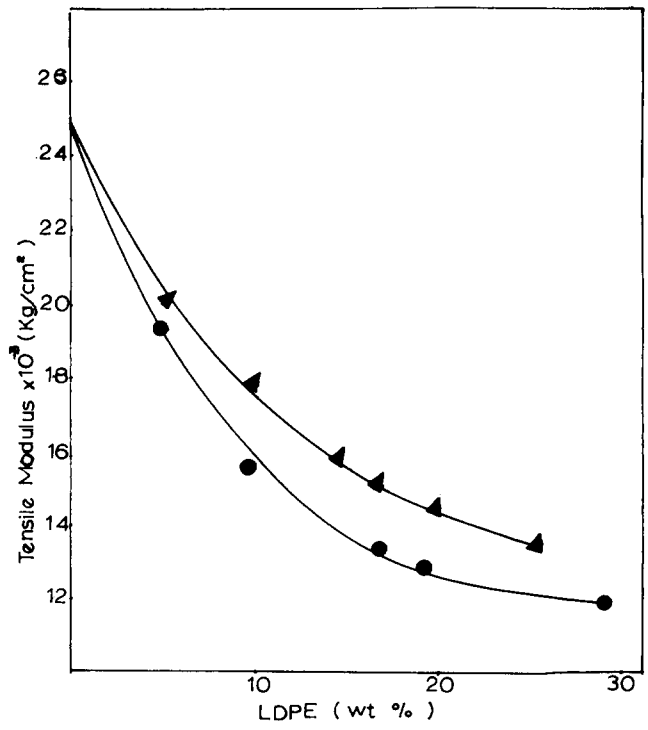

Figure 5 Tensile modulus *versus* weight percentage of LDPE: (▲) PA-6/LDPE; (●) PA-6/LDPE/LDPE-*g*-BuA

LDPE is very low, it contributes very little to the overall modulus when it is dispersed in a PA-6 matrix. From *Figure 5* it can also be inferred that the tensile modulus of all the ternary blends, i.e. PA-6/LDPE/LDPE-*g*-BuA blends, is lower than that of binary blends, i.e. PA-6/LDPE blends. This observation may be ascribed to the fact that in ternary blends, due to the presence of LDPE-*g*-BuA, the system becomes more homogeneous. As a result, more reduction in the tensile modulus is observed.

In *Figure 6*, theoretical predictions of the tensile modulus (see equations (1)–(5)) on the basis of various theories together with the experimental data are given. It can be observed that Nielson's model predicts the data rather well when the value of ϕ_{max} is adjusted. The ϕ_{max} value used for calculating tensile modulus with the aid of equation (3) is given in *Table 2*. A higher value of ϕ_{max} is required when the LDPE content is higher for fitting of experimental results in the Nielson model. It should be noted that a smaller value of ϕ_{max} means a larger volume at the interphase, which is immobilized by the discrete phase in the blend. The reciprocal of ϕ_{max} can be considered as an interaction parameter, which is proportional to $(R + \Delta R/R)^3$ in which R is the radius of the inclusion and ΔR is the depth of interphase that is

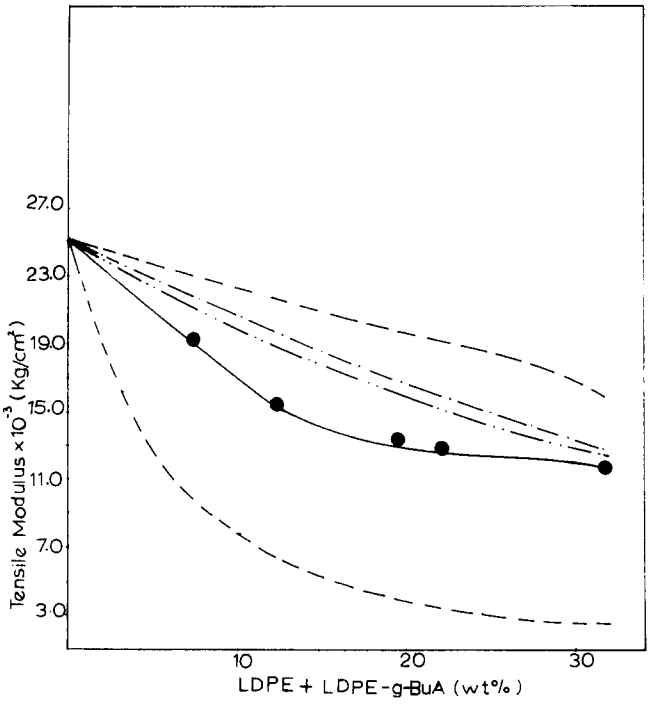

Figure 6 Tensile modulus *versus* weight percentage of LDPE: (●) experimental data; (-----) Paul's upper and lower bounds; (-·-·-) Kerner's model with perfect adhesion; (-··-··-), Kerner's model with loosely bound inclusions; (———) Nielson's model

Table 2 The volume fraction and the maximum packing volume of PA-6/LDPE/LDPE-*g*-BuA blends

Code no.	Volume fraction of PA-6	ϕ_{max}
II	0.91	0.24
III	0.95	0.27
V	0.77	0.42
VI	0.74	0.42
VIII	0.63	0.7

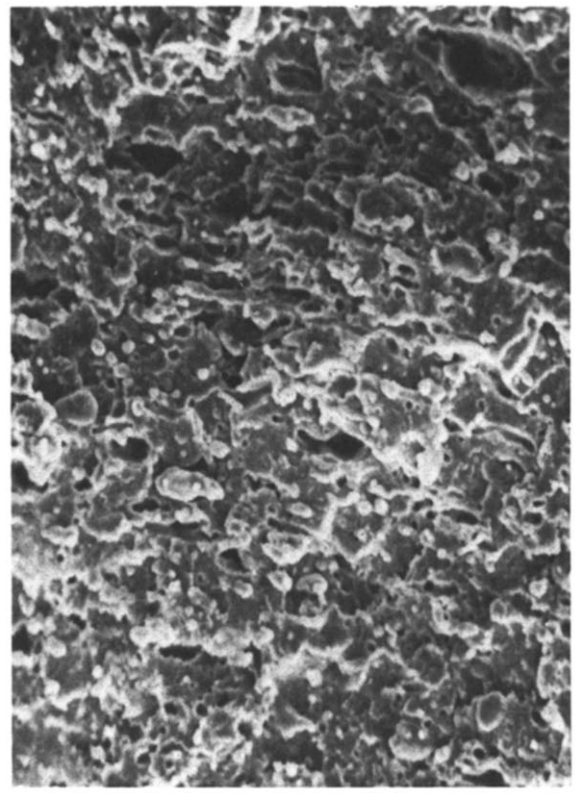

Figure 7 SEM micrograph of an Izod fracture surface of PA-6/LDPE/LDPE-*g*-BuA (IV) blend (200×)

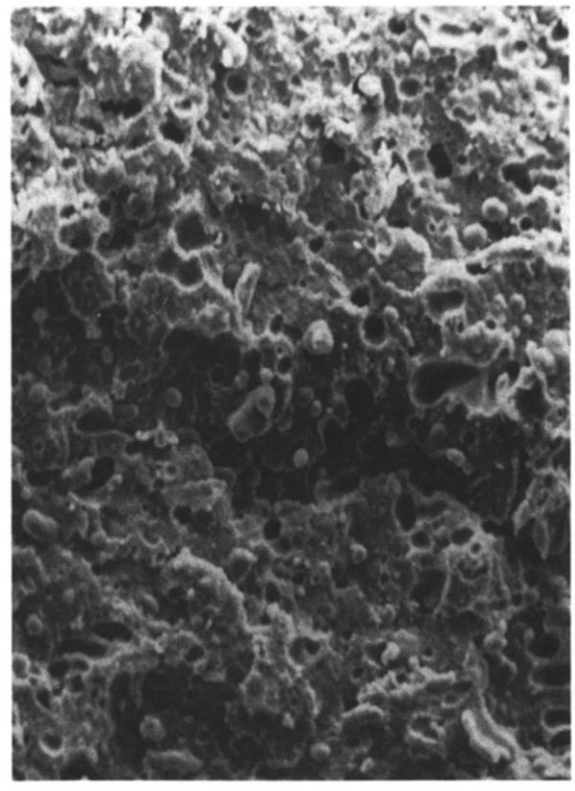

Figure 8 SEM micrograph of an Izod fracture surface of PA-6/LDPE/LDPE-*g*-BuA (VI) blend (200×)

immobilized by the inclusion. For a given value of ΔR, the smaller the size of the inclusion, the smaller the ϕ_{max} value. From *Figures 3*, *7* and *8* it is observed that with increasing LDPE content there is an increase in domain size. Thus the value of ϕ_{max} is expected to be higher with

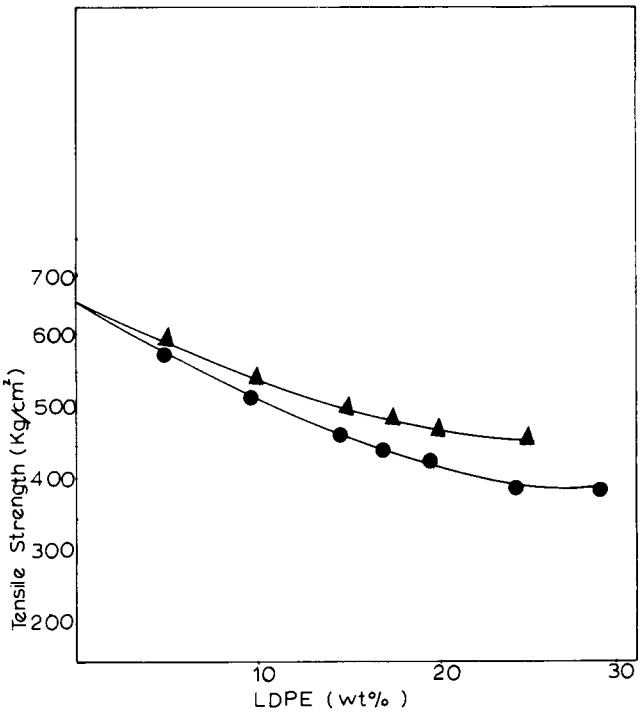

Figure 9 Tensile strength *versus* weight percentage of LDPE: (▲) PA-6/LDPE blends; (●) PA-6/LDPE/LDPE-*g*-BuA blends

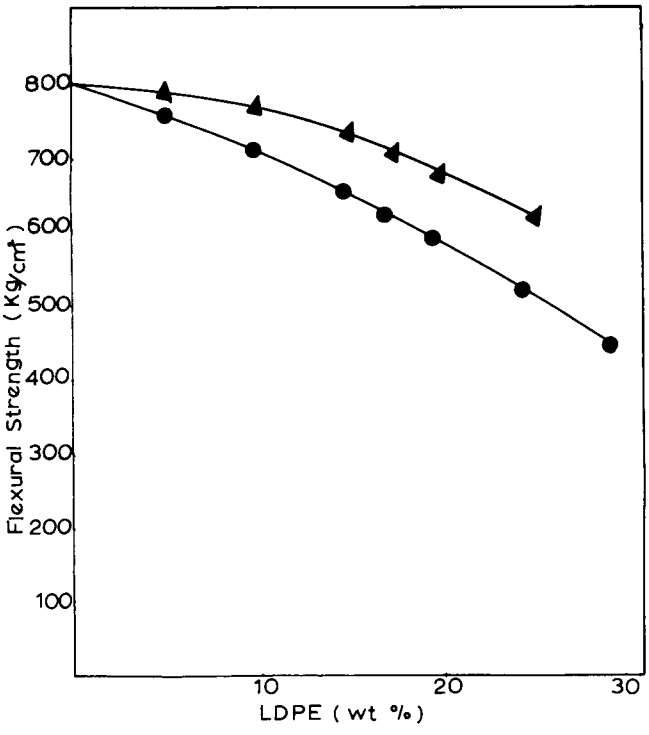

Figure 10 Flexural strength *versus* weight percentage of LDPE; (▲) PA-6/LDPE blends; (●) PA-6/LDPE/LDPE-*g*-BuA blends

increased LDPE content, although the extent of interaction (ΔR) is the same.

From *Figures 9* and *10* it is seen that the tensile strength and flexural strength of all the blends are lower than that of PA-6. This can be attributed to the softening effect due to LDPE addition. From *Figures 9* and *10* it can also be observed that the tensile and flexural strengths of PA-6/LDPE/LDPE-*g*-BuA blends are lower than that of PA-6/LDPE blends. This is probably due to more homogeneity of PA-6/LDPE/LDPE-*g*-BuA blends.

The dependence of the elongation at break on LDPE content is shown in *Figure 11*. This varies a little for the PA-6/LDPE/LDPE-*g*-BuA blends but decreases steeply for PA-6/LDPE blends with increasing LDPE content. The above observation may be ascribed to the fact that for PA-6/LDPE blends the components are incompatible, with almost no mutual adhesion. This is equivalent to the reduction of the transverse area to the tensile direction compared with pure PA-6. Furthermore the large size dispersed particle can probably hinder cold drawing of the PA-6 matrix, causing the premature rupture of material and lowering of the elongation value. Higher values of elongation for PA-6/LDPE/LDPE-*g*-BuA can be explained assuming that PA-6-*g*-LDPE is mostly located at the interface of the PA-6/LDPE, acting as an interfacial agent. Thus higher homogeneity can be achieved with respect to PA-6/LDPE blends. This overall morphology probably contributes to decrease the high stress concentrations around dispersed particles by local plastic deformation and making the system more efficient for cold drawing.

Impact properties

Referring to *Figure 12*, it is observed that PA-6/LDPE exhibits poor impact behaviour. The impact strength of the PA-6/LDPE/LDPE-*g*-BuA initially increases and then decreases with further increase in LDPE content. It can be inferred from *Figures 1* and *2* that in PA-6/LDPE blends dispersed particles have an average diameter of 20 μm and are uniformly distributed throughout the whole sample. It is observed that there is no evidence for adhesion between the PA-6 matrix and the dispersed phase. This morphological observation may explain the lower impact strength.

From *Figures 3*, *7* and *8* it can be observed that the addition of LDPE-*g*-BuA to the binary PA-6/LDPE blends produces a drastic reduction of the average

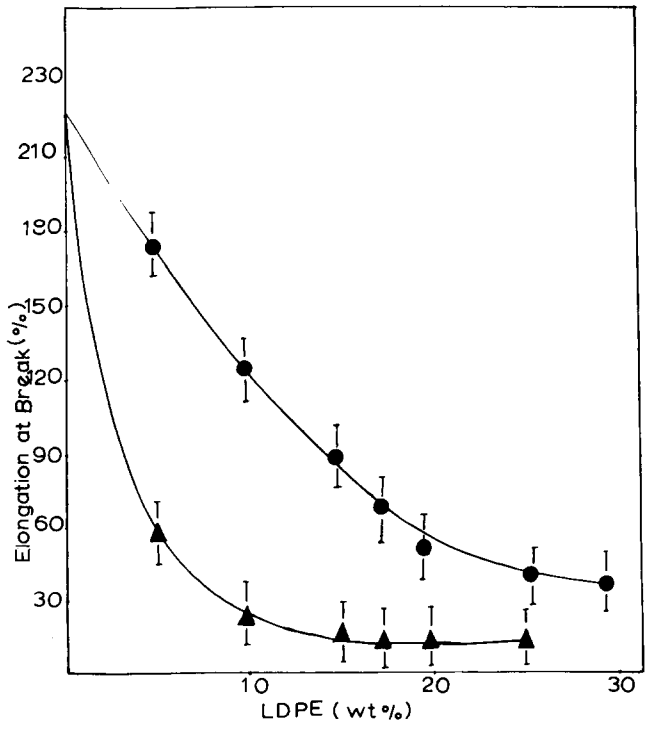

Figure 11 Percentage elongation at break *versus* weight percentage of LDPE: (▲) PA-6/LDPE blends; (●) PA-6/LDPE/LDPE-*g*-BuA blends

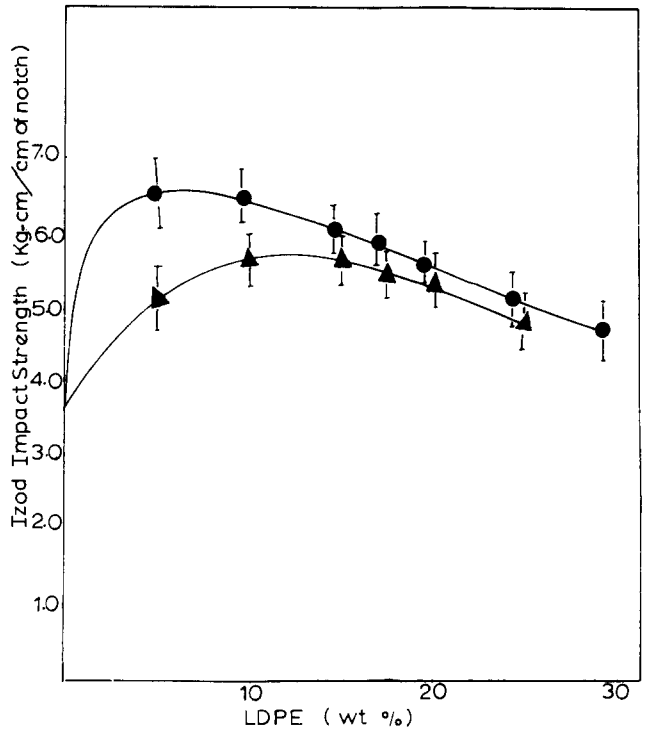

Figure 12 Impact strength *versus* weight percentage of LDPE: (▲) PA-6/LDPE blends; (●) PA-6/LDPE/LDPE-*g*-BuA blends

Table 3 Accuracy and precision of the SEM results

Code no.	Mean diameter for 10 measurements (μm)	Average deviation for 10 measurements	Standard deviation for 10 measurements	Relative standard deviation
II	2.68	0.0018	0.2898	3.42
IV	7.3	0.03	2.211	9.52
VI	10.8	0.012	1.65	4.84

dimensions of the domains of the dispersed phase. The wall cavities are rough, which indicates that adhesion exists between PA-6 matrix and LDPE. As a result the impact strengths of all the blends are higher than that of PA-6. From *Figures 3*, *7* and *8* it is also observed that with increased LDPE content the particle size of the dispersed phase increases (*Table 3*) and adhesion decreases, resulting in a decreased impact strength. From the SEM photographs of the fractured surfaces it is observed that the crack propagates through the matrix (PA-6), and as a result the impact fracture surface of the blends look identical to that of pure PA-6. From this observation we can derive the conclusion that the resulting blends are brittle in nature.

Percentage water absorption

From *Figure 13* it can be inferred that all the blends have lower percentage water absorption values than that of PA-6. As LDPE is insensitive to moisture, all the blends will absorb less moisture. From *Figure 13* it can also be observed that all the ternary blends absorb less water than binary blends. Water susceptibility of PA-6 is mainly due to the presence of amide groups. In PA-6/LDPE/LDPE-*g*-BuA blends, the –C(=O)O– group of butyl acrylate interacts with the amide group. As a result the number of free amide groups in PA-6 is reduced, which reduces the susceptibility of PA-6 for water. The observation can also be taken as an additional indication of the formation of PA-6-*g*-LDPE.

Processability

In *Figure 14* torque *versus* time is plotted for PA-6/LDPE and PA-6/LDPE-*g*-BuA blends. PA-6/LDPE-*g*-BuA shows the higher torque values. This may

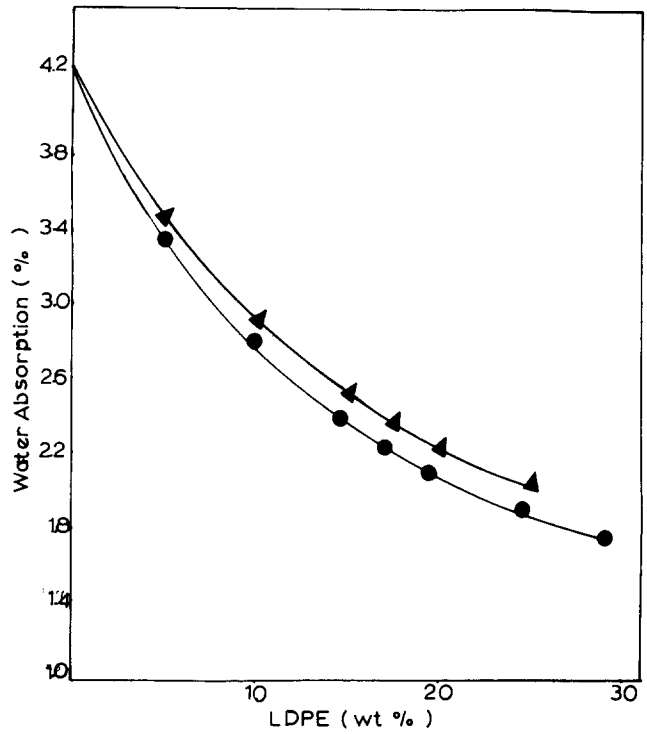

Figure 13 Percentage water absorption *versus* weight percentage of LDPE: (▲) PA-6/LDPE blends; (●) PA-6/LDPE/LDPE-*g*-BuA blends

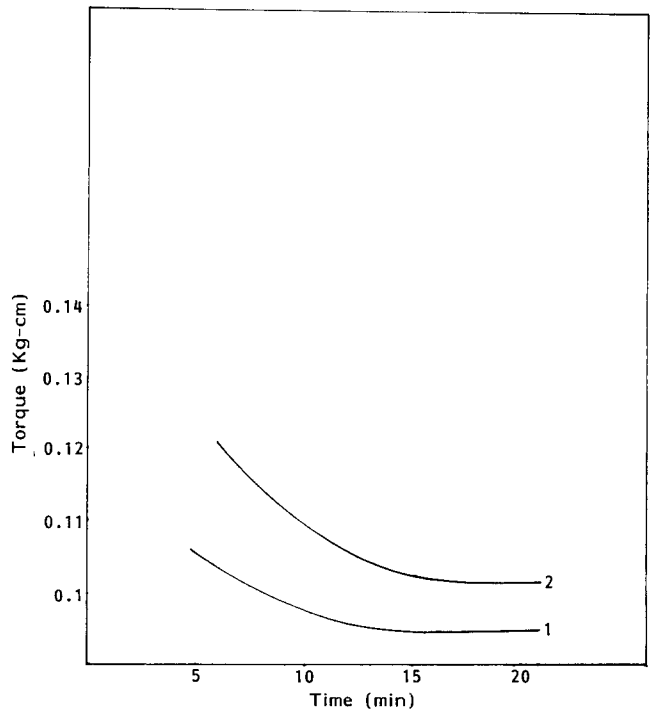

Figure 14 Torque *versus* time: (1) PA-6/LDPE (85/15) blends; (2) PA-6/LDPE-*g*-BuA (85/15) blends

Table 4 Thermomechanical properties of the blends

Code no.	Rockwell hardness (RHR)	*HDT* (°C)	*VST* (°C)
I	115	60	217
II	116	51	212
III	116	52	212
IV	111	51	211
V	110	49	211.5
VI	103	51.5	210
VII	102	50	208
VIII	102	50	208.5
IX	117	51.5	212
X	113	52.5	213
XI	110	51	212
XII	100	51	212
XIII	100	51.5	212
XIV	104	53	209

also be ascribed to the higher homogeneity of PA-6/LDPE-*g*-BuA blends. The increased melt viscosity, i.e. torque value, shows the improved processability of PA-6 and PA-6/LDPE/-*g*-BuA blends.

In *Table 4* the values of heat distortion temperature (*HDT*), Vicat softening temperature (*VST*) and Rockwell hardness *versus* LDPE content for PA-6/LDPE blends and PA-6/LDPE/LDPE-*g*-BuA blends are given. It can be inferred from the table that all the blends have similar Rockwell hardness, *VST* and *HDT* values as that for PA-6. These functions are independent of the nature of LDPE present in the system. As the LDPE has smaller Rockwell hardness, *VST* and *HDT*, it contributes to some extent to overall values of these functions when it is dispersed in the PA-6 matrix. As a result, all the blends have lower *HDT*, *VST* and Rockwell hardness.

CONCLUSIONS

Grafting of butyl acrylate (BuA) onto low-density polyethylene (LDPE) has been carried out by a solution polymerization technique. The resulting LDPE-*g*-BuA has been used as an interfacial agent for polyamide-6 (PA-6)/LDPE blends. All the binary PA-6/LDPE and ternary PA-6/LDPE/LDPE-*g*-BuA blends have been prepared by a melt mixing process. The formation of PA-6-*g*-LDPE graft copolymer during blend preparation has been assumed. Variation in the morphology of the PA-6/LDPE and PA-6/LDPE/LDPE-*g*-BuA blends was observed on changing the LDPE concentration. The tensile properties and impact behaviour of all the prepared blends were investigated and correlated with SEM analysis of the fracture surface. A significant improvement in the impact strength was observed for PA-6/LDPE/LDPE-*g*-BuA blends with percentage composition 92.7/4.9/2.4. In PA-6/LDPE/LDPE-*g*-BuA blends remarkable reduction in the percentage of water absorption with increasing LDPE content was observed. Higher values of torque for PA-6/LDPE-*g*-BuA blends was attributed to the homogeneity of the system. When the value of maximum packing volume is adjusted, the elastic modulus value predicted from the Nielson model was found to match with the experimental value.

REFERENCES

1 Kray, R. J. and Bellet, R. J. Fr. Patent 1470255, 1967
2 Ube Industries Ltd, Jap. Patent 80149312, 1981
3 Mitsubishi Chemical Industries Co. Ltd, Jap. Patent 8208240, 1982
4 Mitsui Petrochemical Industries Ltd, Jap. Patent 6058458, 1985
5 Braun, D. and Eisenlohr, U. *Kunststoffe* 1975, **18**, 139
6 Liang, B., White, J. L., Spruiell, J. E. and Goswami, B. C. *J. Appl. Polym. Sci.* 1983, **28**, 2011
7 Ide, F. and Hasegawa, A. *J. Appl. Polym. Sci.* 1974, **18**, 963
8 Cimino, S., Coppola, F., D'Orazio, L., Greco, R., Maglio, G., Malincomico, M., Mancarella, C., Martuscelli, E. and Ragosta, G. *Polymer* 1986, **27**, 1874
9 Martuscelli, E., Riva, F., Sellitti, C. and Silvestre, L. *Polymer* 1985, **26**, 270
10 Okada, T., Arui, T., Ichikawa, Y. and Tanaka, K. Ger. Patent 3022295, 1981 (*Chem. Abstr.* **94**, 10433a)
11 Takashi, A. Jap. Patent 7596642, 1985
12 Dickie, R. A. in 'Polymer Blends', (Eds. D. R. Paul and S. Newman), Academic Press, New York, 1978, p. 353
13 Kerner, E. H. *Proc. Phys. Soc.* (*B*) 1956, **69**, 808
14 Nielson, N. E. 'Mechanical Properties of Polymer and Composites', Dekker, New York, 1974, Ch. 7
15 Paul, B. *Trans. Metall. Soc. AIME* 1960, **218**, 36
16 Raval, H., Singh, Y. P., Mehta, M. H. and Devi, S. *Polym. Int.* in press
17 Molau, G. E. *J. Polym. Sci.* (*A*) 1965, **3**, 4235